Acoustical Imaging 23
Editor S. Lees and L.A. Ferrari
Plenum Press, New York
to be published

ULTRASONIC REFLECTION TOMOGRAPHY OF POST-DISCOTOMIC SCARRING

A. Pesavento[1], H. Ermert[1], J.Grifka[2], E. Broll-Zeitvogel[2]

[1]Dept. of Electrical Engineering, Ruhr University
[2]Orthopaedische Universitaetsklinik, St. Josefs Hospital
44780 Bochum, Germany

INTRODUCTION

Up to 40% of all back surgery patients suffer from significant post-operative relapsing complaints frequently caused by scarring. Despite modern MR imaging systems there is still al lack of reliable screening diagnostics. Furthermore the image quality of conventional B-scans suffers from low contrast and shadows.

In the past the ultrasound image quality of organs which allow multidirectional scanning like breast, thyroid, and testicles was improved significantly by ultrasonic reflection tomography. With this concept, B-mode images of the same cross sectional object area but from different aspect directions (subimages) are averaged incoherently. While moving the B-scan probe a short distance from the patient's back has to be kept. Therefore, only laterally displaced subimages can be acquired. In order to obtain highly overlapping subimages a sector B-scan system is used.

This way speckle effects and other artifacts are reduced and the image contrast is improved significantly. However, the improvement strongly depends on the decorrelation of the used subimages, whereas the calculation, data acquisition and storage effort rises with every used subimage. Since theoretical derivations of the correlation function of the subimages suffer from approximations that are only valid in the focal region the correlation of the subimages was measured over a wide depth range.

An adaptive compounding system has been developed using the measured correlation functions. The image which is to be compounded is divided into small segment. The segments are compounded using the optimum displacement depending on the considered depth and available subimages. The compounding system was optimized to find a good compromise between the calculation, storage and data acquisition effort and the SNR improvement of the system. The image quality of the system is demonstrated for both, phantom and in vivo images.

SYSTEM SETUP

Figure 1 shows the main components of the compounding system. A conventional B-scan system (Siemens Sonoline SL-2) with a 5 MHz sector scanner is used. The applicator is laterally moved along a line over the patients back by an stepping motor. The RF echo data is acquired by a 30 MHz A/D converter and stored in a PC. TGC and demodulation is done by the compounding software in the PC.

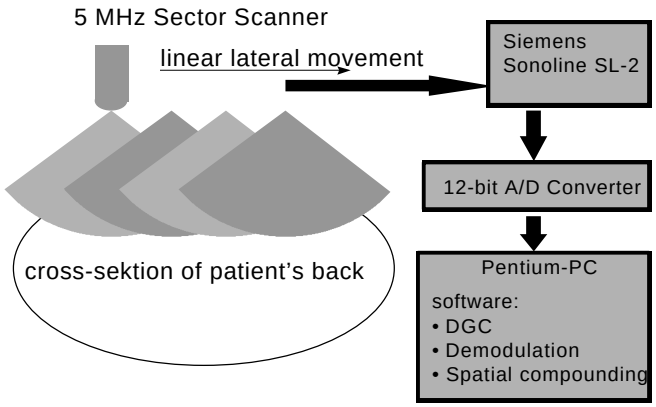

Figure 1. System setup of the applied spatial compounding system

CORRELATION OF SUBIMAGES

Theoretic considerations

The correlation of speckle imaged from different transducer positions has often been subject of research. Burkhardt[1] and later Gehlbach[2] derived the correlation between images formed from different transducer orientations. Subsequent work by Wagner et al.[4,7] following Gehlbach with minor modifications derived a correlation function as a function of lateral transducer shift b using the lateral point spread function $p(x)$,

$$\rho(b) = c\left[\left|FT\left\{|p(x)|^2\right\}\right|^2\right]_{f=2b/\lambda_0 z_0} \qquad (1)$$

with c a constant to assure $\rho(0) = 1$. The result was obtained using monofrequency analysis at the systems center frequency. It assumes that those scatterer which cause echoes are randomly distributed on a line parallel to the transducer instead of being randomly distributed over the resolution cell of the system. Furthermore it assumes the point spread function to be separable into lateral and axial components[4]. Using an approximation of

$$p(x) = \mathrm{sinc}\left(\frac{Dx}{\lambda_0 z_0}\right) = \frac{\sin(\pi Dx/\lambda_0 z_0)}{\pi Dx/\lambda_0 z_0} \qquad (2)$$

with the aperture size D, $\rho(b)$ is depth independent and only depends from the fractional aperture shift b/D. O'Donnell[3] showed that assuming

$$p(x) = A\left(\frac{Dx}{\lambda_0 z_0}\right)\mathrm{sinc}\left(\frac{Dx}{\lambda_0 z_0}\right) \qquad (3)$$

with any beam divergence function $A(z)$ the correlation function $\rho(b)$ in Equation (1) can be analytically solved to a composition of polynomial parts of third order, which is independent from $A(z)$. Despite of the used approximations measurements done by Trahey[5] show good correspondence with this prediction in the focal and far field region. However, the approximations are not valid for a constant focus sector scanner used in our system. Particularly the separation of the point spread function in axial and lateral multiplicative components is only valid for the focal region (because of the rotation of the single transducer). For the same reason the approximation of a sinc function is only valid for sector geometry.

Measurement of the correlation function

Consequently we measured the correlation function over a wide depth range. The measurement was made with a commercially available homogenous speckle phantom.

The correlation of the (sector) image viewed from two different transducer position (1) and (2) was calculated for different image depths d, lateral displacements Dx and aspect angles b (see Figure (2)). The correlation function was found to depend only on the effective lateral displacement $\Delta x' = \Delta x \cos\beta$. This is obvious since the echoes received from transducer position (2) are the same as from an imaginary transducer position (2)' (for small

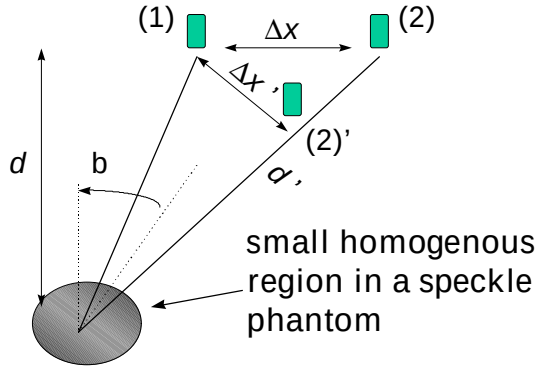

Figure 2. Measurement of speckle correlation

Dx, except of an phase shift, which is irrelevant for the demodulated signals). Considering this, for symmetry reason the correlation function only depends on the distance between the transducer and the imaged region $d' = d / \cos\beta$, not on d and β independently. This agrees with the measurement results. The measured functions were found to be very closely related to exponential functions of the form

$$r(\Delta x', d') = \exp(-\Delta x' / a(d')) \qquad (4)$$

with an depth depended correlation length $\alpha(d')$. However, the correlation length in the focal region of the transducer meets the theoretical predictions of Wagner[4] and O'Donnell[6]. Since the correlation length is only slightly dependent on the depth we used the polynomial fit described in Equation (5) for $\alpha(d')$

$$\alpha(d') = a_0 + a_1 d' + a_2 d'^2 + a_3 d'^3 \qquad (5)$$

The polynomial coefficients a_0, a_1, a_2 and a_3 were estimated using a least square estimator. Therefore the correlation length for the measured depth *d'* had to be estimated using an minimization of the summed absolute differences. The result is presented in Figure 3 showing the single measured correlation lengths and the polynomial fit.

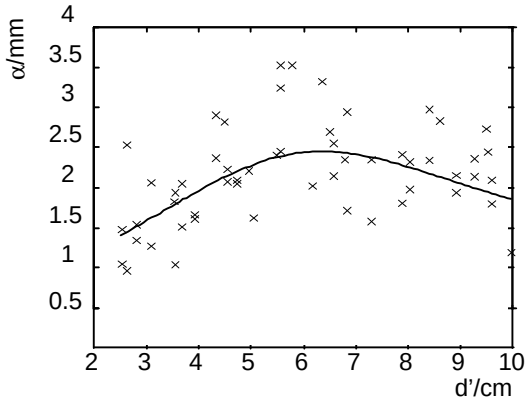

Figure 3. Correlation length α as a function of depth *d'*

The assumption of a sinc-function for the lateral component of the PSF underestimates the lateral resolution in front of the constant focus of the transducer. Applying Equation (1) this leads to a smaller correlation length, which we could confirm with our measurements. Behind the focus the correlation length decreases slightly. This results meets the observations of Trahey[5] and O'Donnell[6].

AN EFFICIENT COMPOUNDING CONCEPT

The SNR of a single ultrasound image with fully developed speckle is known[3] to be approximately 1.91. With spatial compounding this value can be improved[6] to

$$SNR \approx 1.91 N / \sqrt{\sum_{i=1}^{N}\sum_{j=1}^{N} \rho(x_i, x_j)} \qquad (6)$$

where N is the number of used subimages and $\rho(x_i, x_j)$ is the correlation of the subimages viewed from positions x_i, and x_j whereas the SNR improvement for uncorrelated images is proportional to $1/\sqrt{N}$. Due to the speckle correlation, assuming an constant and relatively large acoustical window on the patients back (ca 10 cm) a very dense compounding scheme leads to high acquisition and calculation time but does not lead to a significantly higher SNR than a slightly wider compounding scheme. For very dense compounding schemes the SNR can even fall under an reachable maximum[6,7]. However, since the calculation, data acquisition and storage effort increases with the number of used subimages, a compromise between the effort and the merit of a compounding scheme must be found, meaning an increase of used subimages should lead to an significant increase of the SNR. This compromise can be found by searching the compounding positions x_i that minimize the cost function

$$f(x_i) = N^k / SNR. \qquad (7)$$

Because of the dependence of the SNR on the square root of the number of uncorrelated images, k must be significantly smaller than 0.5. If an value of k=0.5 is taken

the cost function is constant for uncorrelated images. In this work a value of k = 0.35 was chosen.

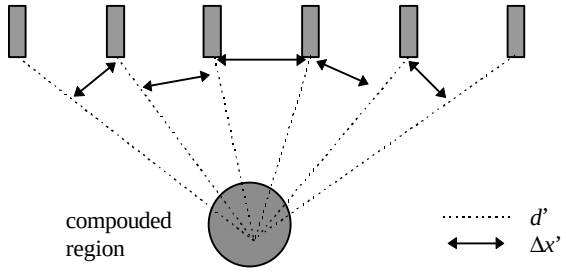

Figure 4. Lateral displacements Δx' and transducer distance d' for an compounding scheme with constant grid

The problem can not satisfactorily be solved by a compounding scheme with constant grid, because the lateral displacements Δx' and transducer distances d' are not constant for neighboring transducer positions. Especially the images viewed from transducer positions with a large angle β are more correlated because of a smaller effective lateral displacement Δx'. For this reason we choose a parametric model for the transducer positions of $x_i = b_0 + b_1 i + b_2 i^2 + b_3 i^3$. The polynom coefficients where found using MATLAB's simplex search method[8], minimizing the cost function Equation (7). Therefore the compounded image was divided into small rectangular segments. For each segment the optimal images to be used where found by the described method. The result was not very much affected by the unavoidable discretisation of the transducer positions which was chosen near the minimum of all the lateral displacements found by the optimization.

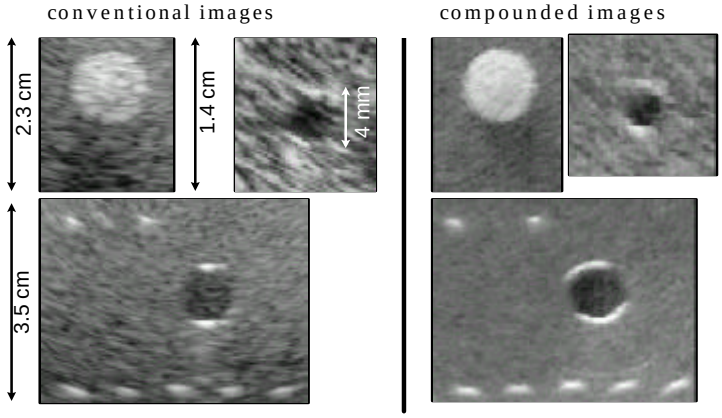

Figure 5. images of a speckle phantom

RESULTS

The SNR improvement of the optimized compounding concept, optimizing cost function Equation (7), was found to be 12 dB in the center segment of the image, with 45 acquired images, assuming an acoustical window of 10 cm. Optimizing the SNR with constant displacement between the subimages (standard compounding concept) a SNR improvement of 12.6 dB can be obtained, with 125 images to acquire. Since some of the acquired images are not used for some segments in the optimized concept, the calculation time increases by a factor of 6.5 for the standard compounding concept. Figure 5 compares images of a speckle phantom produced with the optimized compounding concept with conventional B-mode images of the same areas. Despite of the obvious speckle reduction borders are significantly improved due to the varity of aspect angles.

Figure 6 compares a compounded in vivo image of a human with a conventional one. The images show the back of a post discotomy patient with scarring on the right side. In contrast to the conventional single images the perturbation of the facia due to the operation

is well defined in the compounded image (low echogeneity in region 1) and the asymmetry in the echogeneity of the left and the right side of the processus spinosus with higher echogeneity on the right side indicates the scarring (region 2).

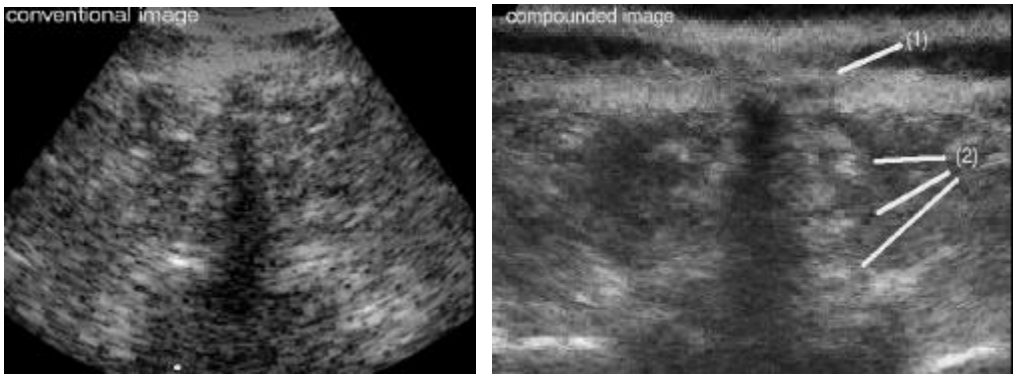

Figure 6. in Vivo images of post discotomic scarring

CONCLUSIONS

Our measurements have shown that in ultrasonic reflection mode tomography the speckle correlation function is depth dependent for a constant focus transducer. For efficient compounding, with a large acoustical window, a segmentwise optimized compounding concept with unequal displacement of the single images minimizes data acquisition and calculation effort by a factor of 6.5 without significant loss of SNR improvement. With the optimized compounding scheme a SNR improvement of approximately 12 dB could be obtained in the center of the image.

ACKNOWLEDGMENTS

This work was supported by the Deutsche Forschungsgemeinschaft, grant Gr 1506/1-1.

REFRENCES

1. C. B. Burckhardt, Speckle in ultrasound B-mode scans, *Trans Sonics Ultrason*. 25:1-6 (1978)
2. S. M. Gehlbach, *Pulse reflection imaging and acoustic speckle*, Ph. D. dissertation, Stanford University, Stanford, CA (1983)
3. R. F. Wagner, S. W. Smith, J. M. Sandrik and H. Lopez, Statistics of Speckle in Ultrasound B-Scans, *Trans. Sonics Ultrason*. 30:156-163 (1983)
4. R. F. Wagner, M. F. Insana and S. W. Smith, Fundamental Correlation Lengths of Coherent Speckle in Medical Ultrasonic Images, *Trans. Ultrason. Ferroelec. Freq. Contr*. 35:34-44 (1988)
5. G. E. Trahey, S. W. Smith and O. T v. Ramm, Speckle Pattern Correlation with Lateral Aperture Translation: Experimental Results an Implications for Spatial Compounding, *Trans. Ultrason. Ferroelec. Freq Contr.* 33:257-264 (1986)
6. M. O'Donnell and S. D. Silverstein, Optimum Displacement for Compound Image Generation in Medical Ultrasound, *Trans. Ultrason. Ferroelec. Freq Contr*. 35:470-476 (1988)
7. A. Lorenz, L. Weng and H. Ermert, A Gaussian Model Approach for the Prediction of Speckle Reduction with Spatial and Frequency Compounding, *Ultrasonic Symposium* (1996)
8. W.H. Press, S.A. Teukolsky, W. T. Vetterling, B.P. Flannery, Numerical Recipes in C, Cambridge Univerity Press, Cambridge (1992)
9. G. Röhrlein, H. Ermert, Limited angle reflection-mode computerized tomography, *Acoustical Imaging* 14:413-424 (1986)
10. D. Hiller, H. Ermert, System analysis of ultrasound reflection mode computerized tomography, *IEEE Trans. Sonics. Ultrason*., 31:240-250 (1984)